

**Interannual summer streamflow variability over Romania  
and its connection to large-scale atmospheric circulation**

Journal:	<i>International Journal of Climatology</i>
Manuscript ID:	JOC-14-0577.R1
Wiley - Manuscript type:	Research Article
Date Submitted by the Author:	08-Jan-2015
Complete List of Authors:	Ionita, Monica; Alfred Wegener Institute, Paleoclimate Dynamics;
Keywords:	streamflow variability, canonical correlation analysis, atmospheric circulation, empirical orthogonal functions, Romania

SCHOLARONE™  
Manuscripts

Peer Review Only

1  
2  
3  
4 1 **Interannual summer streamflow variability over Romania and its connection**  
5 2 **to large-scale atmospheric circulation**  
6  
7  
8 3

9  
10 4 **M. Ionita<sup>1,2</sup>**

11  
12 5 <sup>1</sup> Alfred Wegener Institute Helmholtz Centre for Polar and Marine Research, Bremerhaven, Germany

13  
14 6 <sup>2</sup> MARUM, Bremen University, Bremen, Germany  
15  
16 7

17  
18 8

19  
20 9 Corresponding author:

21  
22  
23 10 Dr. Monica Ionita

24  
25 11 Email: [Monica.Ionita@awi.de](mailto:Monica.Ionita@awi.de)  
26

27  
28 12 Address: Alfred Wegener Institute Helmholtz Centre for Polar and Marine Research

29 13 Bussestrasse 24

30 14 D-27570 Bremerhaven

31 15 Telephone: +49(471)4831-1845

32  
33 16 Fax: +49(471)4831-1271  
34  
35  
36  
37 17  
38  
39 18  
40  
41 19  
42  
43 20  
44  
45 21  
46  
47 22  
48  
49 23  
50  
51 24  
52  
53 25  
54  
55 26  
56  
57  
58  
59  
60

1  
2  
3 27 **Abstract**  
4

5 28 In this study the spatial and temporal variability of summer (June – July – August (JJA))  
6 29 streamflow over Romania, as recorded at 46 hydrological stations over the period 1935 -2010 is  
7 30 analyzed. An empirical orthogonal function analysis (EOFs) and Canonical Correlation Analysis  
8 31 (CCA) were used to characterize the spatial and temporal variability of summer streamflow and  
9 32 the relationship with large-scale atmospheric factors. It is shown that the dominant summer mode  
10 33 captures in-phase variability of river flow anomalies over the entire country, while the second  
11 34 mode of variability is characterized by a northwest - southeast dipole, emphasizing the influence  
12 35 of topography over the streamflow variability. Based on a CCA analysis it is shown that more  
13 36 than 50% of the summer streamflow variability is influenced by cloud cover and summer  
14 37 temperatures, via the modulation of precipitation and potential evapotranspiration. In general,  
15 38 positive (negative) streamflow anomalies, at country level, are associated with cyclonic  
16 39 (anticyclonic) circulation, the advection of moist (warm and dry) air, enhanced (reduced)  
17 40 precipitation and positive (negative) cloud cover anomalies.  
18  
19  
20  
21  
22  
23  
24  
25  
26  
27  
28  
29  
30  
31  
32

33 41

34 42

35 43 KEY WORDS: Romania, atmospheric circulation, streamflow variability, empirical orthogonal functions,  
36 44 canonical correlation analysis  
37 45  
38 46  
39 47  
40 48  
41 49  
42 50  
43 51  
44 52  
45 53  
46 54  
47 55  
48 56  
49 57  
50 58  
51 59  
52 60

## 56 1. Introduction

57 Over the past decades Europe has experienced heavy floods with major consequences for  
58 thousands of people and millions of Euros worth of damage (Kundzewicz et al., 2007). One of  
59 the best examples is the summer 2013 flood in Central Europe which showed how vulnerable  
60 modern society is to hydrological extremes and emphasizes once again the need for improved  
61 forecast methods of such extreme climatic events. In this respect, streamflow forecasting is of  
62 great importance to water resources management and flood defense. On the other hand, to be  
63 able to improve the skill of the streamflow forecast, one needs to get a better understanding of  
64 the streamflow processes and the influence of large scale atmospheric circulation on the  
65 streamflow variability. Characterization of hydrological variability on climatic time scale and  
66 connections to climatic forcings provide potential improvement for hydrological forecasts,  
67 especially if the forcings are predictable or slowly evolving (Souza and Lall, 2003; Croley,  
68 2003). Evidence from long hydrological records shows that periods with anomalous hydrological  
69 behavior (Arnell et al., 1993) are associated with persistent climate anomalies.

70 The interaction between river streamflow and low-frequency climate patterns has been studied  
71 for various hydrological systems all over the world (Dettinger and Diaz, 2000; Barlow et al.,  
72 2001; Barros et al., 2004; Ward et al., 2010). In addition, the analysis of the meteorological-  
73 hydrological connections resulting from synoptic climatic patterns has been suggested to be  
74 essential for understanding and predicting the behavior of river streamflow (Stahl and Demuth,  
75 1999; Bierkens and Van Beek, 2009). Two of the most important phenomena that influence  
76 streamflow variability are the North Atlantic Oscillation (NAO) and El Niño-Southern  
77 Oscillation (ENSO) (Dettinger and Diaz, 2000; Cullen et al., 2002; Lorenzon-Lacruz et al., 2011,  
78 Gamiz-Fortis et al., 2011; Ionita et al., 2008, 2011, 2012). The indices of these two large-scale

1  
2  
3 79 climatic patterns have been used as predictors for the seasonal streamflow anomalies over  
4  
5  
6 80 Europe (Trigo et al., 2002; Rimbu et al.; 2004; Ionita et al., 2008). Correlations with  
7  
8 81 hydrological data have shown that when NAO index is high river flow is above average in the  
9  
10 82 northern part of Europe and below average in the southern part of Europe (Shorthouse and  
11  
12 83 Arnell, 1997; Dettinger and Diaz, 2000). Another atmospheric pattern that strongly influences  
13  
14 84 the precipitation and streamflow over Europe, especially on the southern part, is the East  
15  
16 85 Atlantic/ Western Russia pattern (EA/WR) (e.g. Ziv et al., 2007, Ionita et al., 2014a).  
17  
18  
19 86 Streamflow is an integrated response to climate, water transfer, evapotranspiration and the effect  
20  
21 87 of human activities on the natural water flows. The response time of the streamflow to climate  
22  
23 88 conditions depends strongly on the catchment area characteristics (e.g. geology, topography,  
24  
25 89 soils and vegetation) and among different climatic regions (Post and Jackeman; 1996; Fleig et  
26  
27 90 al., 2011). In the same time, the hydrological response to climate is also season dependent  
28  
29 91 because the water resources, the climatic conditions and the hydrological processes vary  
30  
31 92 throughout the year (Tallaksen, 1995; Garcia-Ruiz et al., 2008).  
32  
33  
34 93 Romania is situated in the southeastern-central part of Europe, north of the Balkan Peninsula and  
35  
36 94 the western shore of the Black Sea. The climatic conditions are dependent on the country's varied  
37  
38 95 topography. The Carpathians serve as a barrier for the Atlantic air masses, limiting their oceanic  
39  
40 96 influences to the west and center of the country, which experience milder winters and heavier  
41  
42 97 rainfalls as a result. The mountains also block the continental influences of the vast plain to the  
43  
44 98 north in the Ukraine, which results in frosty winters and less rain to the south and southeast.  
45  
46 99 Various studies, focused over Romania, have shown certain changes in surface air temperature  
47  
48 100 and precipitation (Bojariu and Paliu, 2001; Tomozeiu et al., 2002; 2005; Ionita et al., 2013,  
49  
50 101 Busuioc et al., 2014). The streamflow variability over this region has been studied only for  
51  
52  
53  
54  
55  
56  
57  
58  
59  
60

1  
2  
3 102 particular regions (Stefan et al., 2004, Rimbu et al., 2004). A first step towards a more  
4  
5 103 comprehensive study, at country level, was made in a recent paper by Ionita et al., (2014b),  
6  
7  
8 104 which showed that the Arctic (AO)/North Atlantic Oscillation (NAO), East Atlantic (EA), East  
9  
10 105 Atlantic/Western Russia (EAWR) and Scandinavian (SCA) patterns control a significant part of  
11  
12 106 the interannual winter streamflow variability over Romania.

13  
14  
15 107 Since the influence of well-known teleconnection patterns, like NAO or El Niño-Southern  
16  
17 108 Oscillation (ENSO), is strongest in winter, most studies which have examined the influence of  
18  
19 109 the atmospheric circulation on the river streamflow are confined to the winter season (Rimbu et  
20  
21 110 al., 2004; Déry and Wood, 2004; Bower et al., 2006; Araneo and Compagnucci, 2008, Ionita et  
22  
23 111 al., 2014b). Only a few studies have examined the variability of river streamflow outside the  
24  
25 112 winter months (Kingston et al., 2006a, b; Ionita et al., 2008, 2011, 2012) over the European  
26  
27 113 region. It has been suggested (Kingston et al., 2006a) that the studies of winter relationship,  
28  
29 114 between streamflow variability and climate related patterns, should not be extrapolated to other  
30  
31 115 seasons, due to the fact that streamflows show a monthly variability both in magnitude and  
32  
33 116 direction (Lawler et al., 2003). As such, the aim of this study is to analyze the spatio-temporal  
34  
35 117 variability of summer streamflow variability over Romania and its relationship with large scale  
36  
37 118 atmospheric circulation based on a country wide data network. The paper is organized as  
38  
39 119 follows: in Section 2 a short description of the data sets and the methods used in this study is  
40  
41 120 given. In Section 3 the main results are presented. The discussion and the main conclusions  
42  
43 121 follow in section 4.  
44  
45  
46  
47  
48  
49  
50

122

123

## 124 2. Data and Methods

125 The streamflow data series used in this study have been provided by the National Institute of  
126 Hydrology and Water Management (INHGA). The time series consist of monthly streamflow  
127 values recorded at 46 stations located over the whole Romanian territory (Figure 1) and cover the  
128 period 1935–2010. The streamflow time series have continuous record and are quality controlled.  
129 Due to the fact that Romania is under the influence of a temperate-continental climate, the  
130 streamflow variability is influenced mainly by the climatic conditions and to a lesser degree by  
131 the topography and regional factors (e.g. geology, vegetation). The streamflow seasonal  
132 variability is determined by the climatic factors, their intensity and frequency (Zavoianu, 2002).  
133 During summer, the streamflow contribution to the annual mean streamflow varies between 15%  
134 in the north-west part of the country up to 30% in the southern and eastern part of the country  
135 (Figure 1b). The high contribution to the annual mean streamflow recorded at the station situated  
136 in the south and eastern part of the country can be the direct results of summer heavy  
137 precipitation events, which are very common for this part of the country (Chelcea and Ionita,  
138 2013).

139 To investigate the relationship of summer streamflow variability with global sea surface  
140 temperature we use the Hadley Centre Sea Ice and Sea Surface Temperature data set (HadISST,  
141 Rayner et al., 2003). This data has a  $2^{\circ} \times 2^{\circ}$  spatial resolution and covers the period 1871–2012. In  
142 the present study we use SST data for the period 1935–2010. For the Northern Hemisphere  
143 atmospheric circulation we used the summer geopotential height at 850mb (Z850), the summer  
144 zonal wind at 850mb (u850) and the summer meridional wind at 850mb (V850) on a  $2^{\circ} \times 2^{\circ}$  grid,  
145 from the Twentieth Century Reanalysis (V2) data (Whitaker et al., 2004; Compo et al., 2006;  
146 Compo et al., 2011), for the period 1935–2010. The temperature at 850 hPa level (TEMP) has

1  
2  
3 147 been extracted from the same data set (Whitaker et al., 2004; Compo et al., 2006; Compo et al.,  
4  
5 148 2011).

6  
7  
8 149 The precipitation (PP), cloud cover (CLD) and Potential Evapotranspiration (PET) data sets were  
9  
10 150 extracted from the gridded data set CRU TS3.1 from the Climatic Research Unit (CRU) of the  
11  
12 151 University of East Anglia (Harris et al., 2013). This data set provides monthly values for various  
13  
14 152 parameters for the global land areas and the temporal coverage is 1901–2012 on a  $0.5^\circ \times 0.5^\circ$   
15  
16 153 grid.

17  
18  
19  
20 154 The dominant patterns of summer streamflow variability are based on Empirical Orthogonal  
21  
22 155 Function (EOF) analysis (e.g. von Storch and Zwiers, 1999). The EOF technique aims at finding  
23  
24 156 a new set of variables that captures most of the observed variance from the data through a linear  
25  
26 157 combination of the original variables. The EOF analysis represents an efficient method to  
27  
28 158 investigate the spatial and temporal variability of time series which cover large areas. This  
29  
30 159 method splits the temporal variance of the data into orthogonal spatial patterns called empirical  
31  
32 160 eigenvectors.

33  
34  
35  
36 161 To identify the coupled summer streamflow and TEMP, CLD and PET patterns we used a  
37  
38 162 Canonical Correlation Analysis (CCA). CCA it is a way of measuring the linear relationship  
39  
40 163 between two multidimensional variables (Preisendorfer, 1988). It identifies two bases, one for  
41  
42 164 each variable, that are optimal with respect to correlations and it finds, at the same time, the  
43  
44 165 corresponding correlations. The same methodology has been applied to study the connection  
45  
46 166 between the summer drought variability over Europe and global SST (Ionita et al., 2012a), the  
47  
48 167 spatial and temporal variability of climate extremes over Romania and their associated large-  
49  
50 168 scale mechanism (Busuioc et al., 2014) and the interannual summer air temperature variability  
51  
52 169 over Greece and its connection to large scale atmospheric circulation (Busuioc et al., 2014). The  
53  
54  
55  
56  
57  
58  
59  
60



1  
2  
3 170 CCA uses as input the output of the EOF analysis (von Storch and Zwiers, 1999) applied to  
4  
5  
6 171 combined standardized anomalies of the predictand (e.g. summer streamflow)/predictors (e.g.  
7  
8 172 TEMP, CLD and PET).  
9

### 10 173 **3. Results**

#### 11 12 13 174 **3.1 Spatio-temporal variability of summer streamflow variability**

14  
15  
16 175 The EOFs resulted from the standardized summer streamflow data set (anomaly divided by  
17  
18 176 standard deviation) allows us to recognize the regions with different streamflow climatology. For  
19  
20 177 this study just the first two EOFs patterns, which together explain more than 71% of the total  
21  
22 178 variance, have been retained. The leading EOF accounts for 60.07% of total variance, while the  
23  
24  
25 179 second EOF accounts for 11.59% of the total variance. These EOF's are well separated according  
26  
27 180 to the North rule (North et al., 1982). The sum of all remaining EOFs adds to ~29% of the total  
28  
29 181 variance.  
30

31  
32 182 The first EOF (Figure 2a) has a monopolar structure showing the same sign for all the analyzed  
33  
34 183 stations, with the highest loadings over the central and northern part of the country. This  
35  
36 184 monopolar structure emphasizes that the streamflow variability over Romania is influenced by  
37  
38 185 the same factors (e.g. the large scale circulation). The corresponding principal component (PC1)  
39  
40 186 presents pronounced interannual and decadal variability (Figure 2b). Positive streamflow  
41  
42 187 anomalies have persisted from the beginning of 1960's up to 1985 and negative streamflow  
43  
44 188 anomalies have persisted from 1985 up to 2010 (Figure 2b). The driest summers (negative  
45  
46 189 streamflow anomalies), in terms of summer PC1, were recorded for the years 1946, 1950, 1999,  
47  
48  
49 190 2003, while the wettest (positive streamflow anomalies) were recorded during the years 1940,  
50  
51  
52 191 1969/1970, 1974/1975, 1980 and 2005, respectively.  
53  
54  
55  
56  
57  
58  
59  
60

1  
2  
3 192 The second EOF pattern (Figure 2c) describes 11.59% of the total variance of the summer  
4  
5 193 streamflow and has a dipole-like structure. This dipole-like structure emphasizes the influence of  
6  
7  
8 194 the Carpathian Mountains on the streamflow variability. This pattern is associated with negative  
9  
10 195 loadings in the north-western part of the country and positive loadings over the south-eastern part  
11  
12 196 of the country. Summer PC2 (Figure 2d) is characterized by enhanced interannual variability  
13  
14 197 with driest summers (negative streamflow anomalies), in terms of summer PC2, recorded for the  
15  
16 198 years 1945, 1974, 1980, 1998, while the wettest summer (positive streamflow anomalies) were  
17  
18 199 recorded during the years 1975, 1991 and 2005, respectively.  
19  
20  
21  
22  
23

### 24 201 **3.2 Coupled modes of variability**

25  
26  
27 202 Before applying a CCA, the dimensionality of the summer streamflow and TEMP, CLD and PET  
28  
29 203 datasets is reduced by an EOF analysis. The first 10 EOF modes of the summer streamflow and  
30  
31 204 the first 11 modes of summer TEMP, CLD and PET are retained as an input into the CCA. The  
32  
33 205 first 10 EOFs capture approximately 92% of the total variance for summer streamflow and more  
34  
35 206 than 87% of the summer TEMP, CLD and PET variability. The optimum number of retained  
36  
37 207 EOFs was chosen so that using one more EOF would not change significantly the canonical  
38  
39 208 correlation (Werner and Von Storch, 1993; Von Storch, 1995). Among other statistical methods,  
40  
41 209 CCA has the advantage to select pairs of optimally correlated spatial patterns, which may lead to  
42  
43 210 a physical interpretation of the mechanism controlling the climate variability (Barnett and  
44  
45 211 Preisendorfer, 1987; Von Storch et al., 1993; Von Storch, 1995). This multivariate approach is  
46  
47 212 increasingly being used in the atmospheric sciences as well, investigating climate data,  
48  
49 213 geophysical fields, and ocean-atmosphere relationships (e.g., Barnston and Ropelewski 1992;  
50  
51 214 Bretherton et al. 1992; Ionita et al., 2012; Busuioc et al. 2014).  
52  
53  
54  
55  
56  
57  
58  
59  
60

1  
2  
3  
4 215 Figure 3 shows the first CCA mode associated with summer streamflow variability over  
5  
6 216 Romania. The first CCA pattern, referred from now on as CCA1, which explains 52.31% of the  
7  
8 217 total variance of summer streamflow variability and 13.226% of the three predictors' fields, has a  
9  
10 218 monopolar structure with high positive loadings at all the analyzed stations (Figure 3a). The first  
11  
12 219 canonical mode associates simultaneously positive streamflow anomalies all over the country,  
13  
14 220 negative PET (Figure 3c) and TEMP (Figure 3d) anomalies and positive CLD (Figure 3e)  
15  
16 221 anomalies over the whole central and southern part of Europe, with the highest values of  
17  
18 222 coefficients over Hungary and the northwestern part of Romania. From Figure 3 is obvious that  
19  
20 223 positive streamflow anomalies, at country level, are very sensitive to the thermodynamic  
21  
22 224 contributions coming from TEMP, PET and CLD. Similar results have been found by Busuioc et  
23  
24 225 al. (2014) which showed that the extreme summer precipitation over Romania is mostly sensitive  
25  
26 226 to thermodynamic factors (e.g. TEMP and specific humidity at 700mb) compared to the  
27  
28 227 dynamics factors (e.g. sea level pressure). The spatial structure of CCA1 for summer streamflow  
29  
30 228 resembles the structure of summer EOF1 (Figure 2a). The year to year variations of the  
31  
32 229 normalized temporal components of the first CCA pairs are presented in Figure 3b. The two time  
33  
34 230 series (TS1 streamflow and TS1 predictors) are significantly correlated ( $r = 0.80$ ) and have a  
35  
36 231 temporal behavior similar to summer PC1 (Figure 2b). The two canonical time series present  
37  
38 232 strong variability both on interannual as well as on decadal time scale.  
39  
40 233 The second CCA pair, referred from now on as CCA2, exhibits a correlation between the time  
41  
42 234 series corresponding to the summer streamflow (TS2) and the predictors of  $r = 0.57$ . The  
43  
44 235 explained variance of CCA2 corresponding to the summer streamflow is 9.31%, while for the  
45  
46 236 three predictors is 11.15%, respectively. The second CCA pattern (Figure 4a) has a more  
47  
48 237 regional distribution compared to CCA1. For the summer streamflow, the highest positive  
49  
50  
51  
52  
53  
54  
55  
56  
57  
58  
59  
60

1  
2  
3 238 loadings are found over the central and eastern part of Romania (the extra-Carpathian region),  
4  
5 239 while the north-western part of the country (the intra-Carpathian region) is characterized by  
6  
7  
8 240 negative, but smaller loadings (Figure 4a). Positive streamflow anomalies over the central and  
9  
10 241 eastern part of the country are associated with weak positive PET (Figure 4c) and TEMP (Figure  
11  
12 242 4d) anomalies and negative CLD (Figure 4e) anomalies over these regions. Compared to CCA1,  
13  
14 243 the loadings of PET, TEMP and CLD are much smaller, implying the fact that other factors  
15  
16 244 might play a more important role in the variability of the second CCA streamflow mode. The  
17  
18 245 second pair of canonical temporal series (Figure 4b) presents mostly interannual variability and a  
19  
20 246 shift towards more positive values at the beginning of the 1970's.  
21  
22  
23

### 24 247 **3.3 Relationship with large scale atmospheric circulation and sea surface temperature**

25  
26  
27  
28 248 To identify the physical mechanism responsible for the connection between the summer  
29  
30 249 streamflow variability as identified by the CCA and large-scale atmospheric circulation we  
31  
32 250 constructed the composite maps between the first two principal components corresponding to the  
33  
34 251 first two canonical modes (TS1 and TS2) of the summer streamflow and Z850 and wind vectors  
35  
36 252 at 850mb for the years of **High** (TS > 0.75 std. dev.), respectively **Low** (TS < -0.75 std. dev.)  
37  
38 253 values of the normalized times series of the TSs. This threshold was chosen as a compromise  
39  
40 254 between the strength of the climate anomalies associated to flow anomalies and the number of  
41  
42 255 maps which satisfy this criteria. Further analysis has shown that the results are not sensitive to  
43  
44 256 the exact threshold value used for our composite analysis (not shown). Moreover, in this sub-  
45  
46 257 section the relationship between the summer streamflow variability and precipitation (PP) and  
47  
48 258 the North Atlantic Ocean SST is analyzed in terms of correlation maps between the first two TSs  
49  
50 259 and summer PP and summer SST. The results of the correlation analysis are shown in Figure 5 (c)  
51  
52  
53  
54  
55  
56  
57  
58  
59  
60

1  
2  
3 260 and d) and Figure 6 (c and d), in which the correlations that are exceeding the 95% significance  
4  
5 261 level are hatched.

6  
7  
8 262 The composite map of Z850 anomalies and the wind vectors at 850mb for the years  
9  
10 263 characterized by high values of TS1 ( $TS1 > 0.75$  std. dev.) shows a dipole-like structure, with  
11  
12 264 positive Z850 anomalies over the British Isle, North Sea and Scandinavian Peninsula and a deep  
13  
14 265 center of negative Z850 anomalies centered over the eastern part of Europe (Figure 5a). The  
15  
16 266 negative Z850 anomalies centered over the eastern part Europe are consistent with enhanced  
17  
18 267 precipitation (Figure 5c) over this region and the advection of moist air from the Mediterranean  
19  
20 268 region (Figure 5d) towards Romania (see the wind vectors in Figure 5a) and as a consequence  
21  
22 269 high streamflow anomalies all over the Romanian territory. For the years characterized by  
23  
24 270 negative values of TS1 ( $TS1 < -0.75$ std) the composite maps of Z850 anomalies and the wind  
25  
26 271 vectors at 850mb is characterized by a wave train with positive Z850 anomalies over the eastern  
27  
28 272 coast of U.S. and western North Atlantic, negative Z850 anomalies over the eastern Atlantic  
29  
30 273 Ocean, positive Z850 anomalies over the eastern part of Europe and negative Z850 anomalies  
31  
32 274 over Russia (Figure 5b). This kind of pattern favors the advection of dry and warm air from the  
33  
34 275 south-eastern part of Europe towards Romania and reduced precipitation and hence low  
35  
36 276 streamflow anomalies. The Z850 and wind anomalies patterns identified for TS1 are in full  
37  
38 277 agreement with the results found in the previous section. In general, positive (negative)  
39  
40 278 streamflow anomalies, at country level, are associated with cyclonic (anticyclonic) circulation,  
41  
42 279 the advection of cold and moist (warm and dry) air, enhanced (reduced) precipitation and  
43  
44 280 positive (negative) CLD. Positive streamflow anomalies over the entire country (positive TS1  
45  
46 281 values) are also associated with enhanced precipitation at the country level (Figure 5c) and an  
47  
48  
49  
50  
51  
52  
53  
54  
55  
56  
57  
58  
59  
60

1  
2  
3 282 SST pattern characterized by positive SST anomalies over the tropical Atlantic Ocean and the  
4  
5  
6 283 central part and negative SST anomalies over the Mediterranean Sea (Figure 5d).  
7  
8 284 The composite map of Z850 anomalies for the years characterized by high TS2 values ( $> 0.75$   
9  
10 285 std. dev.) shows a different structure compared to the case of summer TS1 (Figure 6a). Positive  
11  
12 286 streamflow anomalies over the central and eastern part of Romania and negative streamflow  
13  
14 287 anomalies over the western part of Romania are associated with a wave-train in the Z850 field  
15  
16 288 characterized by positive Z850 anomalies over the western coast of North Atlantic Ocean,  
17  
18 289 negative Z850 anomalies over Greenland, positive Z8500 anomalies over the British Isle, North  
19  
20 290 Sea and the Scandinavian Peninsula and negative Z850 anomalies over the southern part of  
21  
22 291 Europe. In this case the south-eastern part of Romania is under the action of cyclonic activity,  
23  
24 292 most probably coming from the Mediterranean region, which is known to be a region of intense  
25  
26 293 cyclonic development. This Z850 pattern is associated with strong advection of warm and dry air  
27  
28 294 from the north-eastern part of the continent towards the western part of Romania (low  
29  
30 295 streamflow) and warm and humid air from the Black Sea towards the southern and eastern part  
31  
32 296 of the country and enhanced precipitation (Figure 6c). The composite map of Z850 anomalies for  
33  
34 297 the years characterized by low ( $< -0.75$  std. dev.) TS2 values (Figure 6b) features also a wave-  
35  
36 298 train like structure, with negative Z850 anomalies over the western coast of the Atlantic Ocean  
37  
38 299 extending up to the northern part of Europe and the Scandinavian Peninsula flanked on the north  
39  
40 300 side by positive Z850 anomalies all over Greenland and on the southern part by positive Z850  
41  
42 301 anomalies over the northern part of Africa and southern part of Europe. The anticyclonic activity  
43  
44 302 over the southern part of Europe causes reduced precipitation and low streamflow over the  
45  
46 303 southern and central part of Romania, while the cyclonic activity over the central Atlantic and  
47  
48 304 the northern part of European enhances precipitation over the western part of Romania. High  
49  
50  
51  
52  
53  
54  
55  
56  
57  
58  
59  
60

1  
2  
3 305 streamflow over the southern and central part of Romania and low streamflow over the western  
4  
5 306 part (positive values of TS2) are associated with an SST pattern characterized by negative SST  
6  
7 307 anomalies over the tropical Atlantic and south of Greenland and positive SST anomalies over the  
8  
9 308 European coast and the Mediterranean Sea (Figure 6d). The SST from the Mediterranean Sea has  
10  
11 309 a strong influence on the development of the cyclonic activity over this area (Quereda et al.,  
12  
13 310 2011), which in turns affects the streamflow variability especially over the southern and central  
14  
15 311 part of Romania. Warm SSTs in summer, especially over the western part of the Mediterranean  
16  
17 312 Sea (where the positive correlations between TS2 and summer SST are) are associated with  
18  
19 313 explosive cyclogenesis (Quereda et al., 2011) due to the fact that positive SST anomalies over  
20  
21 314 this area stand as highly convective surfaces with respect to the overlying air. In agreement with  
22  
23 315 our findings, in a recent study Vespreamu-Stroe et al (2012) have shown that the wind regime  
24  
25 316 over the Romanian territory, especially over the south-eastern part, is strongly influenced by the  
26  
27 317 cyclogenesis in the Mediterranean region. They showed that enhanced cyclogenesis over the  
28  
29 318 Mediterranean region induces positive winds anomalies and storm occurrences especially over  
30  
31 319 the south-eastern part of Romania (where the highest loadings of CCA2 are found).  
32  
33  
34  
35  
36  
37  
38  
39  
40

## 41 5. Discussion and conclusions

42  
43  
44 322 In summary, in this study we have investigated the spatio-temporal variability of the summer  
45  
46 323 streamflow over Romania and its relationship with large-scale atmospheric circulation and global  
47  
48 324 SST. There is a lack of studies that assess this relationship, especially over Romania, and the  
49  
50 325 existing ones are either restricted to different parts of the country (Stefan et al., 2005) or just over  
51  
52 326 a single catchment area (Rimbu et al., 2004). The only study made at country level, has been  
53  
54 327 recently published by Ionita et al. (2014b). In this study it is shown that different climate modes  
55  
56  
57  
58  
59  
60

1  
2  
3 328 of variability (e.g. AO/NAO, EA, EAWR and SCA) control a significant part of the interannual  
4  
5 329 winter streamflow variability over Romania. The aim of the current study was to analyze the  
6  
7  
8 330 variability of summer streamflow and identify the main triggers of this variability. The results  
9  
10 331 obtained here differ significantly from the ones obtained for the winter season. This is not so  
11  
12 332 surprisingly, if one takes into account that the influence of well-known teleconnection patterns is  
13  
14 333 strongest in winter and less visible in summer (Kingston et al., 2006a). In this study it is shown  
15  
16 334 that the variability of summer streamflow is influenced by atmospheric circulation patterns that  
17  
18 335 do not project onto any well-know teleconnection patterns and most of this variability is strongly  
19  
20 336 influenced by variations in summer temperature, cloud cover and potential evapotranspiration.  
21  
22 337 A large part of the summer streamflow variability is explained by a monopolar structure, both for  
23  
24 338 the EOF analysis as well as for the CCA analysis, suggesting that more than 60% (explained  
25  
26 339 variance of summer EOF1) of the summer streamflow is driven by the same mechanism via the  
27  
28 340 large-scale atmospheric circulation. The summer streamflow variability over Romania is  
29  
30 341 characterized by dry summers (negative streamflow anomalies) for the period 1940 up to 1965  
31  
32 342 and 1985 up to 2009 and wet summers (positive streamflow anomalies) for the period 1965 up to  
33  
34 343 1984. The second mode of summer variability (EOF2) is characterized by a dipole-like structure  
35  
36 344 and emphasizes the influence of the Carpathian Mountains, being more sensitive to  
37  
38 345 regional/local factors, like topography.  
39  
40 346 The CCA experiments with the combined large-scale predictors and summer streamflow served  
41  
42 347 to investigate the co-variability between PET, TEMP, CLD and the Romanian streamflow for a  
43  
44 348 network of 46 stations, at country level. The first coupled mode (CCA1) emphasizes that more  
45  
46 349 than 52% of the total summer streamflow variability can be explained by a linear combination of  
47  
48 350 PET, TEMP and CLD. Positive streamflow anomalies, at country level, are associated with  
49  
50  
51  
52  
53  
54  
55  
56  
57  
58  
59  
60



1  
2  
3 351 negative PET and TEMP anomalies and positive CLD anomalies. Our results are in full  
4  
5  
6 352 agreement with previous studies which showed that for the spring and summer seasons, an  
7  
8 353 increase in air temperature is associated with reduced precipitation, which can be the result of  
9  
10 354 reductions of cloudiness (Tang et al., 2010). The increase in temperature could be further  
11  
12 355 enhanced by soil moisture reduction, which in turn reduces the evaporation and evaporative  
13  
14 356 cooling on the surface. Based on the aforementioned results we can argue that cloud and  
15  
16 357 temperature forcings are determinant for more than 50% of the summer streamflow variability,  
17  
18 358 throughout the modulation of summer precipitation and evapotranspiration. Similar results have  
19  
20 359 been found recently by Busuioc et al. (2014) which showed that the variability of summer  
21  
22 360 temperature and precipitation extremes is controlled by the thermodynamic factors, via TEMP  
23  
24 361 and specific humidity at 700hPa level. In general, positive (negative) streamflow anomalies, at  
25  
26 362 country level, are associated with cyclonic (anticyclonic) circulation, the advection of cold and  
27  
28 363 moist (warm and dry) air, enhanced (reduced) precipitation and positive (negative) CLD.  
29  
30  
31  
32  
33 364 Global warming is expected to result in substantial changes in streamflow and thus affect the  
34  
35 365 water supplies management (IPCC, 2013). Since more than 50% of the summer streamflow  
36  
37 366 variability was found to be influenced by the thermodynamic factors and taking into account the  
38  
39 367 projected increase in the mean temperature, especially over the southern part of Europe (IPCC,  
40  
41 368 2013) one could expect an increase in the water resources scarcity in the future over these  
42  
43 369 regions. In agreement with these findings, Barsan et al. (2014) have shown that the summer  
44  
45 370 streamflow over the extra-Carpathian region shows a decreasing trend in the last 35 years and  
46  
47 371 they speculated that this decreasing trend is related to the increase in the mean air temperature at  
48  
49 372 country level.  
50  
51  
52  
53  
54  
55  
56  
57  
58  
59  
60

1  
2  
3 373 The second CCA mode of summer streamflow variability presents strong interannual variability  
4  
5 374 and more local characteristics. The relationship with PET, TEMP and CLD persists, but the  
6  
7  
8 375 amplitudes of the canonical modes are much smaller compared to the first mode. For the second  
9  
10 376 canonical mode the Carpathian Mountains have a strong influence on the summer streamflow  
11  
12 377 variability. CCA2 shows an opposite relationship between the summer streamflow and PET,  
13  
14  
15 378 TEMP and CLD when compared to CCA1, especially over the extra-Carpathian regions. Positive  
16  
17 379 summer streamflow anomalies over the extra-Carpathian regions are associated with weak  
18  
19  
20 380 positive TEMP and PET anomalies over the southern part of Romania. This contrasting  
21  
22 381 relationship can be explained via the *Clausius-Clapeyron* relation. Due to increased temperature,  
23  
24 382 model projections show that rainfall will become more intense, mostly due to the presence of  
25  
26  
27 383 more moisture in the atmosphere (IPCC, 2014). The projections show an increase in the intensity  
28  
29 384 of precipitation, but a decrease in the frequency of precipitation events. As such, an increase in  
30  
31 385 the temperature could lead to more intense precipitation and hence floods, yet to longer dry  
32  
33  
34 386 periods between two rain events and hence droughts (IPCC, 2013). This could explain the  
35  
36 387 contrasting relationship between the summer streamflow and TEMP and PET for CCA1 and  
37  
38  
39 388 CCA2, especially over the south-eastern part of Romania which is very sensitive to changes in  
40  
41 389 temperature and evapotranspiration. Busuioc et al. (2014) have shown also that positive TEMP  
42  
43 390 and specific humidity anomalies, with the highest magnitude over the southern part of Romania,  
44  
45  
46 391 are associated with negative anomalies of extreme dry periods, which is in agreement with the  
47  
48  
49 392 results identified for CCA2.

50  
51 393 In general, negative (positive) streamflow anomalies on the northwestern (south and south-  
52  
53 394 eastern) part of the country are associated with reduced (enhanced) precipitation over the  
54  
55 395 northwestern (south and south-eastern) part of Romania as a response to the influence of large-

1  
2  
3 396 scale atmospheric circulation and Atlantic Ocean and the Mediterranean SST. Negative  
4  
5 397 (positive) summer streamflow anomalies over the northwestern (south and south-eastern) part of  
6  
7  
8 398 the country are associated with anticyclonic (cyclonic) circulation which in turn favors the  
9  
10 399 advection of warm and dry (humid and warm air) from the eastern part of the continent  
11  
12  
13 400 (Mediterranean Sea).

14  
15 401 The results shown here help to understand the variability of the summer streamflow conditions  
16  
17 402 over Romania and identify possible mechanism behind this variability. In conclusion, we have  
18  
19  
20 403 shown that the streamflow variability over Romania is strongly related to large-scale atmospheric  
21  
22 404 patterns and this kind of analysis can be useful to connect long-term hydrological variability to  
23  
24 405 climate forcings. In agreement with previous studies (e.g. Tang et al., 2010; Tang and Leng,  
25  
26  
27 406 2012, Busuioc et al., 2014) we show that a large part of the summer streamflow variability is  
28  
29 407 very sensitive to cloud and temperature forcings. Such an analysis provides a useful tool to find  
30  
31 408 meaningful physical mechanism which can explain the changes in the regime of streamflow  
32  
33  
34 409 variability. Moreover, the characterization of the climate influence on the streamflow variability  
35  
36 410 could provide a useful basis for the construction of statistical or dynamical prediction models for  
37  
38 411 the evolution of streamflow, which in turn could lead to a better water resources management, at  
39  
40  
41 412 country level.

42  
43 413

44  
45 414

46  
47 415

48  
49 416

50  
51 417

52  
53 418

419 **References**

420

421 Araneo DC, Compagnucci RH. 2008. Atmospheric circulation features associated to Argentinean Andean  
422 rivers discharge variability, *Geophys. Res. Lett.* **35**: L01805, doi:10.1029/2007GL032427.

423 Arnell NW, Krasovskaia I, Gottschalk L. 1993. River flow regimes in Europe. In Flow Regimes from  
424 International Experimental and Network Data (FRIEND), vol. 1. *Hydrological Studies, Gustard A*  
425 *(ed.)*. Institute of Hydrology: Wallingford, Oxfordshire, UK : 112-121.

426 Barlow M, Nigam S, Berbery EH. 2001. ENSO, Pacific Decadal Variability, and U.S. Summertime  
427 Precipitation, Drought, and Stream Flow. *J. Climate.* **14**: 2105–2128.

428 Barnett TP, Preisendorfer R. 1987. Origin and levels of monthly and seasonal forecast skill for United  
429 States surface air temperatures determined by canonical correlation analysis. *Mon. Wea. Rev.* **115**:  
430 1825–1850.

431 Barnston AG, Ropelewski CF. 1992. Prediction of ENSO episodes using canonical correlation analysis. *J.*  
432 *Climate.* **5**: 1316-1345.

433 Barros V, Chamorro L, Coronel G, Baez J. 2004. The Major Discharge Events in the Paraguay River:  
434 Magnitudes, Source Regions, and Climate Forcings. *J. Hydrometeorol.* **5**: 1161–1170.

435 Birsan MV, Zaharia L, Chendes V, Branescu E. 2014. Seasonal trends in Romanian streamflow. *Hydrol.*  
436 *Process.* **28**: 4496–4505. doi: 10.1002/hyp.9961

437 Bojariu R, Paliu D. 2001. North Atlantic Oscillation projection on Romanian climate fluctuations in the  
438 cold season, Detecting and Modelling Regional Climate Change and Associated Impacts, M.  
439 Brunet and D. Lopez eds., Springer-Verlag , 345-356.

440 Bouwer LM, Vermaat JE, Aerts JCJH. 2006. Winter atmospheric circulation and river discharge in  
441 northwest Europe, *Geophys. Res. Lett.* **33**: L06403, 10.1029/2005GL025548.

442 Bretherton C, Smith C, Wallace JM. 1992. An intercomparison of methods for finding coupled patterns  
443 in climate data. *J. Climate.* **5**: 541-560.

- 1  
2  
3 444 Busuioc A, Dobrinescu A, Birsan MV, Dumitrescu A, Orzan A. 2014. Spatial and temporal variability of  
4  
5 445 climate extremes in Romania and associated large-scale mechanisms. *Int. J. Climatol.*,  
6  
7 446 doi: 10.1002/joc.4054.  
8  
9  
10 447 Chelcea S, Ionita M. 2013. Extreme value analysis of the Barlad river time series, "OVIDIUS" University  
11  
12 448 annals – Constanta, year XIV– issue 15 (2013), series: Civil Engineering, Section VII. Hydrology  
13  
14 449 and Hydrogeology. Environment Protection, pp. 273 – 280, ISSN 1584-5990, Ovidius University  
15  
16 450 Press, Constanța, Romania.  
17  
18 451 Compo GP, Whitaker JS, Sardeshmukh PD, Matsui N, Allan RJ, Yin X, Gleason BE, Vose RS, Rutledge  
19  
20 452 G, Bessemoulin P, Brönnimann S, Brunet M, Crouthamel RI, Grant AN, Groisman PY, Jones PD,  
21  
22 453 Kruk M, Kruger AC, Marshall GJ, Maugeri M, Mok HY, Nordli Ø, Ross TF, Trigo RM, Wang  
23  
24 454 XL, Woodruff SD, Worley SJ. 2011. The Twentieth Century Reanalysis Project. *QJR Meteorol.*  
25  
26 455 *Soc.* **137**: 1-28. DOI: 10.1002/qj.776.  
27  
28  
29 456 Compo GP, Whitaker JS, Sardeshmukh PD. 2006. Feasibility of a 100 year reanalysis using only surface  
30  
31 457 pressure data. *Bull. Amer. Met. Soc.* **87**: 175-190.  
32  
33 458 Croley TE II, Luukkonen CL. 2003. Potential Effects of Climate Change on Ground Water in Lansing,  
34  
35 459 Michigan. *Journal of the American Water Resources Association* **39**: 149-163.  
36  
37  
38 460 Cullen HM, Kaplan A, Arkin P, DeMenocal PB. 2002. Impact of the North Atlantic Oscillation on  
39  
40 461 Middle Eastern climate and streamflow. *Clim. Change* **55**: 315– 338.  
41  
42 462 Déry SJ, Wood EF. 2004. Teleconnection between the Arctic Oscillation and Hudson Bay river discharge.  
43  
44 463 *Geophys. Res. Lett.* **31**, L18205, doi:10.1029/2004GL020729.  
45  
46  
47 464 Dettinger MD, Diaz HF. 2000. Global characteristics of streamflow seasonality. *Journal of*  
48  
49 465 *Hydrometeorology.* **1**: 289– 310.  
50  
51 466 Fleig AK, Tallaksen LM, Hisdal H, Hannah DM. 2011. Regional hydrological drought in north-western  
52  
53 467 Europe: linking a new regional drought area index with weather types. *Hydrol. Process.* **25**:  
54  
55 468 1163–1179.  
56  
57  
58  
59  
60

- 1  
2  
3 469 Gámiz-Fortis SR, Hidalgo-Muñoz JM., Argüeso D, Esteban-Parra MJ, aCastro-Díez Y. 2011. Spatio-  
4  
5 470 temporal variability in Ebro river basin (NE Spain): global SST as potential source of  
6  
7 471 predictability on decadal time scales, *J. Hydrol.* **409**: 759–775.
- 9  
10 472 García-Ruiz JM, Regüés D, Alvera B, Lana-Renault N, Serrano-Muela P, Nadal-Romero E, Navas A,  
11  
12 473 Latron J, Martí-Bono C, Arnáez J. 2008. Flood generation and sediment transport in experimental  
13  
14 474 catchments affected by land use changes in the central Pyrenees. *J. Hydrol.* **356 (1–2)**: 245–260.
- 16 475 Harris I, Jones PD, Osborn TJ, Lister DH. 2013. Updated high-resolution grids of monthly climatic  
17  
18 476 observations. *Int. J. Climatol.* **34**: 623–642. doi: 10.1002/joc.3711
- 20 477 Ionita M., Lohmann G., Rimbu N. 2008. Prediction of Elbe discharge based on stable teleconnections  
21  
22 478 with winter global temperature and precipitation, *J Climate* **21**: 6215 - 6226.  
23  
24 479 DOI:10.1175/2008JCLI2248.1
- 27 480 Ionita M, Rimbu N, Lohmann G. 2011. Decadal variability of the Elbe river streamflow. *International*  
28  
29 481 *Journal of Climatology* **31 (1)**: 22–30. DOI: 10.1002/joc.2054.
- 31 482 Ionita M, Lohmann G, Rimbu N, Chelcea S, Dima M. 2012a. Interannual to decadal summer drought  
32  
33 483 variability over Europe and its relationship to global sea surface temperature. *Clim. Dyn.* **38(1–**  
34  
35 484 **2)**:363–377.
- 37 485 Ionita M, Lohmann G, Rimbu N, Chelcea S. 2012b. Interannual Variability of Rhine River Streamflow  
38  
39 486 and Its Relationship with Large-Scale Anomaly Patterns in Spring and Autumn. *J. Hydrometeor.*  
40  
41 487 **13**: 172–188.
- 44 488 Ionita M, Rimbu N, Chelcea S, Patrut S. 2013. Multidecadal variability of summer temperature over  
45  
46 489 Romania and its relation with Atlantic Multidecadal Oscillation, *Theor. Appl. Climatol.* **113**: 305  
47  
48 490 – 315. doi: 10.1007/s00704-012-0786-8.
- 50 491 Ionita M. 2014a. The impact of the East Atlantic/Western Russia pattern on the hydroclimatology of  
51  
52 492 Europe from mid-winter to late spring, *Climate* **4**: 296-309.
- 54  
55  
56  
57  
58  
59  
60

- 1  
2  
3 493 Ionita M, Chelcea S, Rimbu N, Adler MJ. 2014b. Spatial and temporal variability of winter streamflow  
4  
5 494 over Romania and its relationship to large-scale atmospheric circulation. *Journal of Hydrology*.  
6  
7 495 DOI: 10.1016/j.jhydrol.2014.09.024  
8  
9  
10 496 IPCC. 2013. Climate Change 2013: The Physical Science Basis. Contribution of Working Group I to the  
11  
12 497 Fifth Assessment Report of the Intergovernmental Panel on Climate Change [Stocker TF, Qin D,  
13  
14 498 Plattner GK, Tignor M, Allen SK, Boschung J, Nauels A, Xia Y, Bex V, Midgley PM (eds.)].  
15  
16 499 Cambridge University Press, Cambridge, United Kingdom and New York, NY, USA, 1535 pp,  
17  
18 500 doi:10.1017/CBO9781107415324  
19  
20 501 Kingston DG, Lawler DM, McGregor GR. 2006a. Linkages between atmospheric circulation, climate and  
21  
22 502 streamflow in the northern North Atlantic: research prospects. *Progress in Physical Geography*  
23  
24 503 **30(2)**: 143–174.  
25  
26  
27 504 Kingston DG, McGregor GR, Hannah DM, Lawler DM. 2006b. River flow teleconnections across the  
28  
29 505 northern North Atlantic margin. *Geophysical Research Letters* **33**: L14705.  
30  
31 506 DOI:10.10292006/GL026574.  
32  
33  
34 507 Kundzewicz ZW, Mata LJ, Arnell N, Döll P, Kabat P, Jiménez B, Miller K, Oki T, Şen Z, Shiklomanov I.  
35  
36 508 2007. Freshwater resources and their management. Climate Change 2007: Impacts, Adaptation  
37  
38 509 and Vulnerability. Contribution of Working Group II to the Fourth Assessment Report of the  
39  
40 510 Intergovernmental Panel on Climate Change (ed. by M. L. Parry, O. F. Canziani, J. P. Palutikof,  
41  
42 511 P. J. van der Linden & C. E. Hanson), 173–210. Cambridge University Press, UK  
43  
44 512 <http://www.ipcc.ch/pdf/assessment-report/ar4/wg2/ar4-wg2-chapter3.pdf>.  
45  
46  
47 513 Lawler DM, McGregor GR, Phillips ID. 2003. Influence of atmospheric circulation changes and regional  
48  
49 514 climate variability on river flow and suspended sediment fluxes in southern Iceland. *Hydrol.*  
50  
51 515 *Process* **17(16)**: 3195–3223.  
52  
53  
54 516 Lorenzo-Lacruz J, Vicente-Serrano SM, López-Moreno JI, González-Hidalgo JC, Morán-Tejeda E. 2011.  
55  
56 517 The response of Iberian rivers to the North Atlantic Oscillation, *Hydrol. Earth Syst. Sci.* **15**: 2581-  
57  
58 518 2597, doi:10.5194/hess-15-2581-2011.  
59  
60

- 1  
2  
3 519 North GR, Bell TL, Cahalan RF, Moeng FJ. 1982. Sampling errors in the estimation of empirical  
4  
5 520 orthogonal functions, *Mon. Wea. Rev.* **110**(7): 699-706.  
6  
7 521 Post DA, Jakeman AJ. 1996. Relationships between catchment attributes and hydrological response  
8  
9 522 characteristics in small Australian mountain ash catchments. *Hydrol. Process.* **10**: 877–892  
10  
11 523 Preisendorfer RW. 1988. *Principal Component Analysis in Meteorology and Oceanography*. Amsterdam:  
12  
13 524 Elsevier, 425 pp.  
14  
15 525 Quereda J, Monton E, Escrig J. 2011. Teleconnections between the North Atlantic SST and  
16  
17 526 Mediterranean rainfall. *Tethys* **8**: 31–42, DOI:10.3369/tethys.2011.8.04  
18  
19 527 Rayner NA, Parker DE, Horton EB, Folland CK, Alexander LV, Rowell DP, Kent EC, Kaplan A. 2003.  
20  
21 528 Global analyses of sea surface temperature, sea ice, and night marine air temperature since the  
22  
23 529 late nineteenth century. *J. Geophys. Res.* **108**: No. D14, 4407 10.1029/2002JD002670  
24  
25 530 Rimbu N, Dima M, Lohmann G, Stefan S. 2004. Impacts on the North Atlantic Oscillation and the El  
26  
27 531 Niño-Southern Oscillation on Danube river flow variability. *Geophysical Research Letters* **31**:  
28  
29 532 L23203, doi:10.1029/2004GL020559.  
30  
31 533 Shorthouse CA, Arnell NW. 1997. Spatial and temporal variability in European river flows and the North  
32  
33 534 Atlantic oscillation, in: *Regional Hydrology – Concepts and models for sustainable water*  
34  
35 535 *management, IAHS*.  
36  
37 536 Souza Filho FA, Lall U. 2003. Seasonal to interannual ensemble streamflow forecasts for Ceara, Brazil:  
38  
39 537 Applications of a multivariate, semiparametric algorithm, *Water Resources Research* **39**: 1307.  
40  
41 538 DOI:10.1029/2002WR001373.  
42  
43 539 Stefan S, Ghioca M, Rimbu N, Boroneant C. 2004. Study of meteorological and hydrological drought in  
44  
45 540 southern Romania from observational data. *Int. J. Climatol.* **24**: 871–881. doi: 10.1002/joc.1039  
46  
47 541 Tallaksen LM. 1995. A review of baseflow recession analysis. *J. Hydrol.* **165**: 349–370.  
48  
49 542 Tang Q, Leng G, Groisman PY, 2012. European Hot Summers Associated with a Reduction of  
50  
51 543 Cloudiness. *J Climate* **25**: 3637–3644  
52  
53  
54  
55  
56  
57  
58  
59  
60



- 1  
2  
3 544 Tang Q, Guoyong L. 2012. Damped summer warming accompanied with cloud cover increase over  
4  
5 545 Eurasia from 1982 to 2009, *Environ. Res. Lett.* **7** 014004  
6  
7 546 Tomozeiu R, Busuioc A, Stefan S. 2002. Changes in seasonal mean of maximum air temperature in  
8  
9 547 Romania and their connection with large-scale circulation. *Int J Climatol.* **22**:1181-1196.  
10  
11 548 Tomozeiu R, Stefan S, Busuioc A. 2005. Winter precipitation variability and large-scale circulation  
12  
13 549 patterns in Romania. *Theor Appl Climatol.* doi:10.1007/s00704-004-0082-3.  
14  
15  
16 550 Trigo RM, Osborn TJ, Corte-Real JM. 2002. The North Atlantic Oscillation influence on Europe: climate  
17  
18 551 impacts and associated physical mechanisms, *Clim. Res.* **20**: 9 – 17.  
19  
20 552 Verpreamu-Stroe A, Cheval S, Tatui F. 2012. The wind regime of Romania – Characteristics, trends and  
21  
22 553 North Atlantic Influences. *Forum Geografic* 12/2012; XI (2):118-126. DOI: 10.5775/fg.2067-  
23  
24 554 4635.2012.003.d  
25  
26  
27 555 Von Storch H. 1995. Spatial Patterns: EOFs and CCA. In: Analysis of climate variability: application of  
28  
29 556 statistical techniques (eds. H. Von Storch and A. Navarra). Springer Verlag, 227–258.  
30  
31 557 Von Storch H, Zwiers FW. 1999. Statistical Analysis in Climate Research. Cambridge University Press,  
32  
33 558 494 pp.  
34  
35  
36 559 Ward PJ, Beets W, Bouwer LM, Aerts JCJH., Renssen H. 2010. Sensitivity of river discharge to ENSO,  
37  
38 560 *Geophys. Res. Lett.* **37**: L12402, doi:10.1029/2010GL043215 .  
39  
40 561 Werner P, Von Storch H. 1993. Interannual variability of Central European mean temperature in January–  
41  
42 562 February and its relation to large–scale circulation, *Clim. Res.* **3**: 195–207.  
43  
44 563 Whitaker JS, Compo GP, Wei X, Hamill TM. 2004. Reanalysis without radiosondes using ensemble data  
45  
46 564 assimilation. *Mon. Wea. Rev.* **132**: 1190-1200.  
47  
48  
49 565 Xoplaki E, González-Rouco JF, Gyalistras D, Luterbacher J, Rickli R, Wanner H. 2003. Interannual  
50  
51 566 summer air temperature variability over Greece and its connection to the large-scale atmospheric  
52  
53 567 circulation and Mediterranean SSTs 1950-1999. *Clim. Dyn.* **20**: 537-554.  
54  
55 568 Zavoianu I. 2002. Hidrologie, editia a II-a, Ed. Fundatiei Romania de Maine, 2002, ISBN 973-582-456-6  
56  
57  
58  
59  
60

1  
2  
3  
4  
5  
6  
7  
8  
9  
10  
11  
12  
13  
14  
15  
16  
17  
18  
19  
20  
21  
22  
23  
24  
25  
26  
27  
28  
29  
30  
31  
32  
33  
34  
35  
36  
37  
38  
39  
40  
41  
42  
43  
44  
45  
46  
47  
48  
49  
50  
51  
52  
53  
54  
55  
56  
57  
58  
59  
60

569 Ziv B, Dayan U, Kushnir Y, Roth C, Enzel Y. 2006. Regional and global atmospheric patterns governing  
570 rainfall in the southern Levant. *Int. J. Climatol.* **26**: 55–73.

571  
572  
573  
574  
575  
576  
577  
578  
579  
580  
581  
582  
583  
584  
585  
586  
587  
588  
589  
590  
591  
592  
593  
594

Peer Review Only

1  
2  
3 595 **Figure captions**  
4  
5  
6 596  
7

8 597 **Figure 1.** a) The topographic map of Romania and the location of the stations used in this study;  
9  
10 598 b) The contribution (%) of summer streamflow to the mean annual streamflow for the 46  
11  
12 599 streamflow over Romania for the 1935-2010 period.

13 600  
14 601 **Figure 2.** a) First EOF (EOF1) of summer (June/July/August - JJA) streamflow; b) the  
15  
16 602 corresponding time series (PC1) and the 7years running mean (black line); c) The second EOF  
17  
18 603 (EOF2) of summer (June/July/August - JJA) streamflow; d) The corresponding time series (PC2)  
19  
20 604 the 7years running mean (black line). For PC1 and PC2 time series the units are standardized  
21  
22 605 anomalies.

23 606  
24  
25 607 **Figure 3.** a) The spatial pattern of the first CCA (CCA1) of the summer streamflow; b) The  
26  
27 608 normalized time components of CCA1: TS1 streamflow (black line) and TS1 predictors (red  
28  
29 609 line); c) The spatial pattern of the first CCA (CCA1) of the summer PET; d) The spatial pattern  
30  
31 610 of the first CCA (CCA1) of the summer TEMP and e) The spatial pattern of the first CCA  
32  
33 611 (CCA1) of the summer CLD.

34 612  
35  
36 613 **Figure 4.** a) The spatial pattern of the second CCA (CCA2) of the summer streamflow; b) The  
37  
38 614 normalized time components of CCA1: TS1 streamflow (green line) and TS1 predictors  
39  
40 615 (magenta line); c) The spatial pattern of the second CCA (CCA2) of the summer PET; d) The  
41  
42 616 spatial pattern of the second CCA (CCA2) of the summer TEMP and e) The spatial pattern of the  
43  
44 617 second CCA (CCA2) of the summer CLD.

45 618  
46  
47 619 **Figure 5.** a) The **High** ( $TS1 > 0.75$  std. dev.) composite map between summer streamflow TS1  
48  
49 620 and summer Geopotential Height at 850 mb ( $Z_{850}$  – shaded areas) and summer 850mb Wind  
50  
51 621 vectors (arrows); b) The **Low** ( $TS1 < -0.75$  std. dev.) composite map between summer  
52  
53 622 streamflow TS1 and summer Geopotential Height at 850 mb ( $Z_{850}$  – shaded areas) and summer  
54  
55 623 850mb Wind vectors (arrows); c) The correlation map between summer streamflow TS1 and  
56  
57 624 summer PP; d) The correlation map between summer streamflow TS1 and summer SST. The  
58  
59 625 dotted areas indicate regions where the correlations are exceeding the 95% significance level.

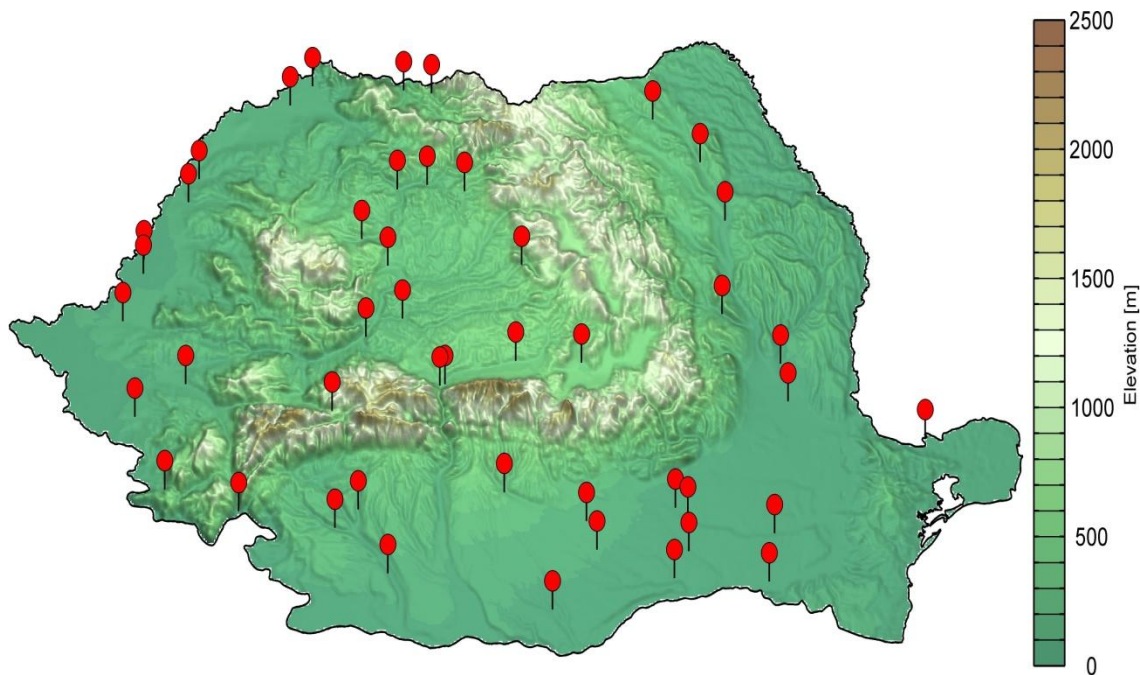
1  
2  
3  
4 626 **Figure 6.** a) The **High** ( $TS2 > 0.75$  std. dev.) composite map between summer streamflow TS2  
5 627 and summer Geopotential Height at 850 mb (Z850 – shaded areas) and summer 850mb Wind  
6 628 vectors (arrows); b) The **Low** ( $TS2 < -0.75$  std. dev.) composite map between summer  
7 629 streamflow TS2 and summer Geopotential Height at 850 mb (Z850 – shaded areas) and summer  
8 630 850mb Wind vectors (arrows); c) The correlation map between summer streamflow TS2 and  
9 631 summer PP; d) The correlation map between summer streamflow TS2 and summer SST. The  
10 632 dotted areas indicate regions where the correlations are exceeding the 95% significance level.  
11  
12  
13  
14  
15

16 633

17 634

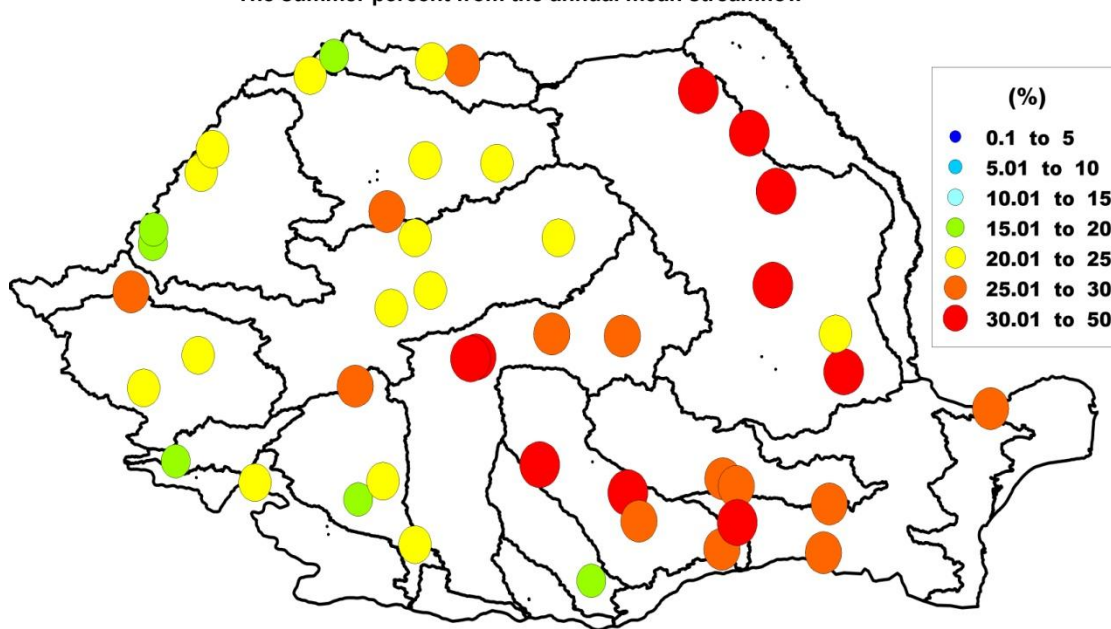
18 635  
19  
20  
21  
22  
23  
24  
25  
26  
27  
28  
29  
30  
31  
32  
33  
34  
35  
36  
37  
38  
39  
40  
41  
42  
43  
44  
45  
46  
47  
48  
49  
50  
51  
52  
53  
54  
55  
56  
57  
58  
59  
60

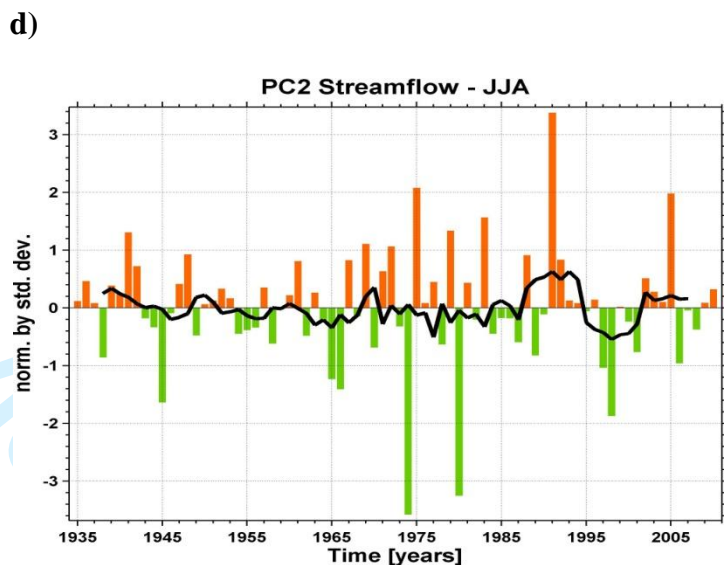
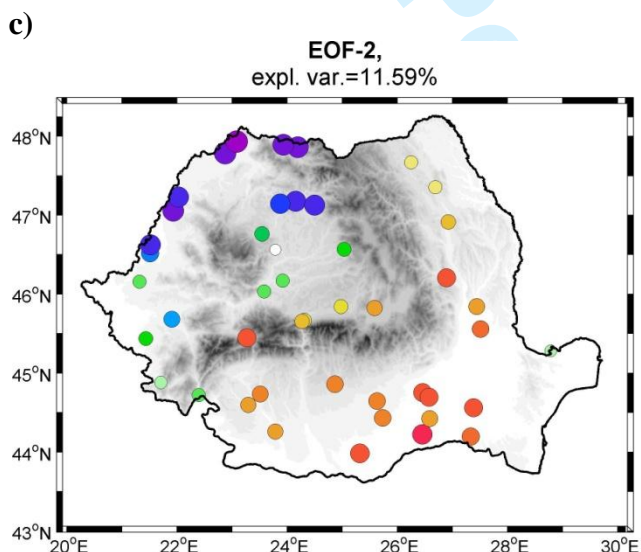
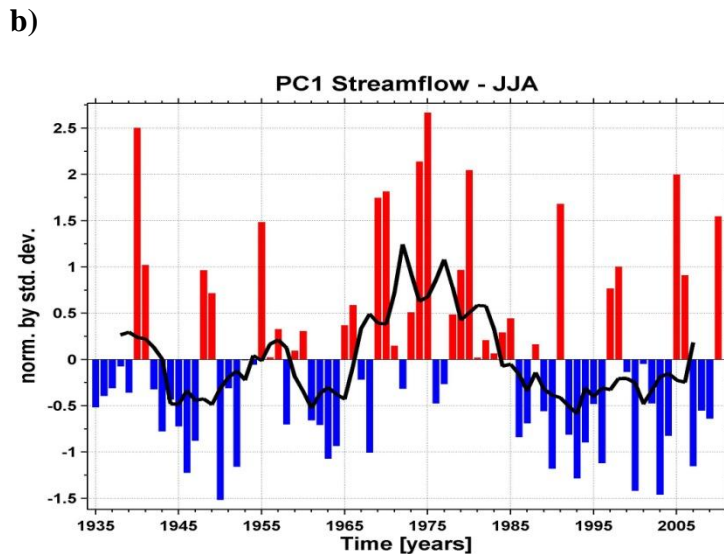
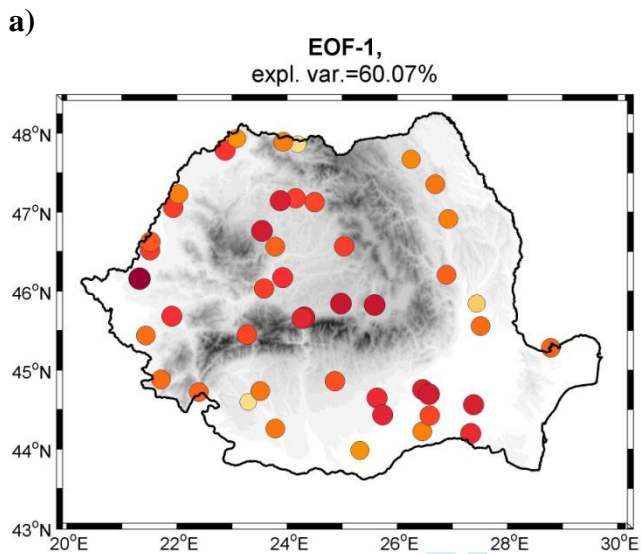
a)



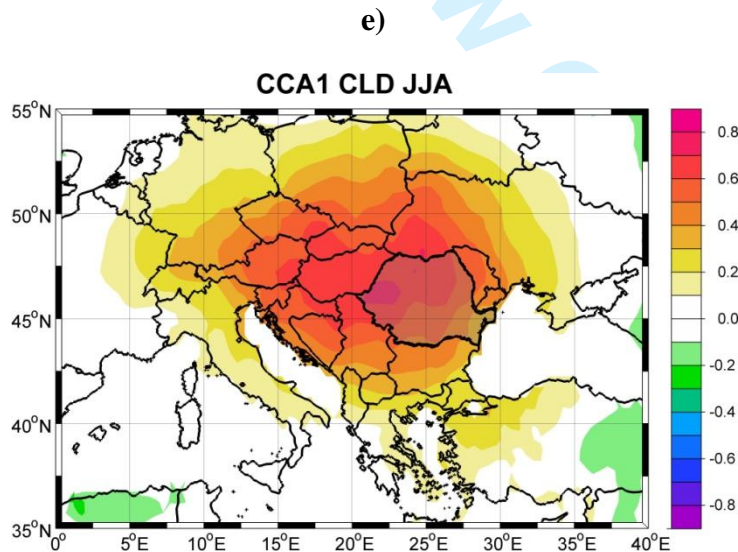
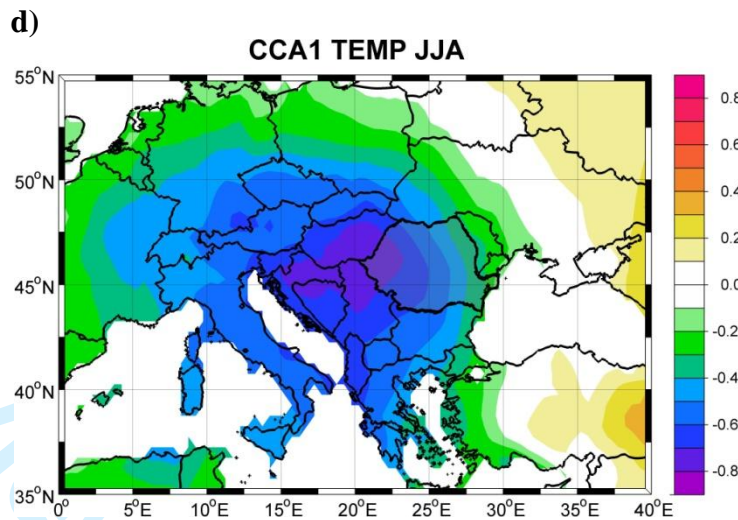
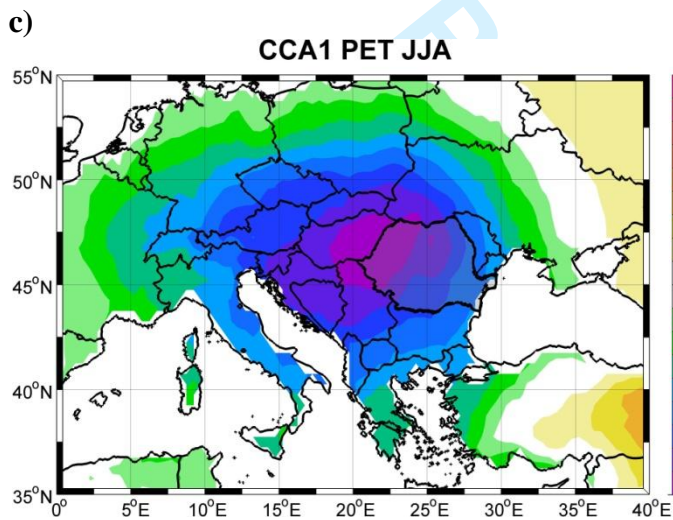
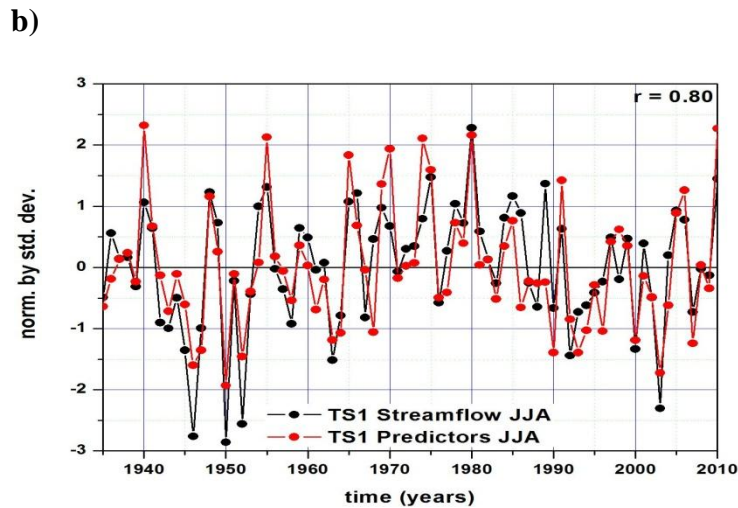
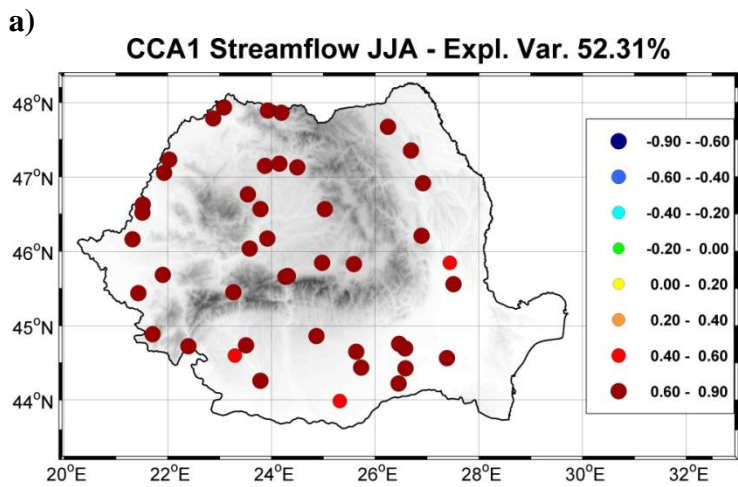
b)

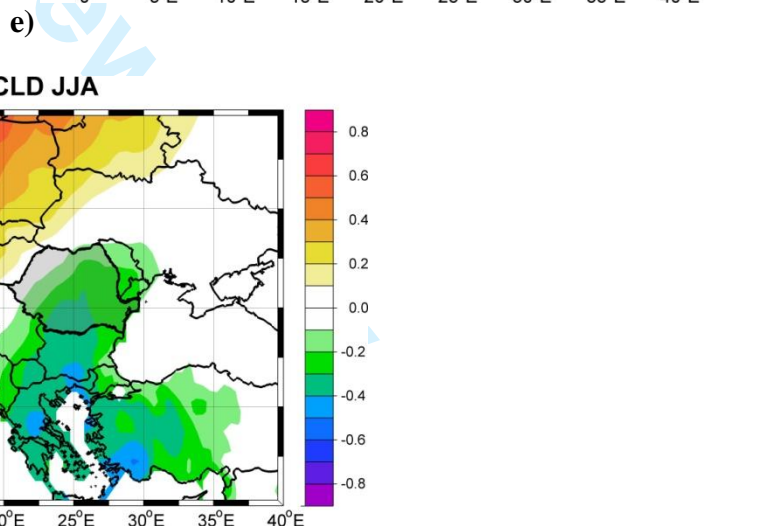
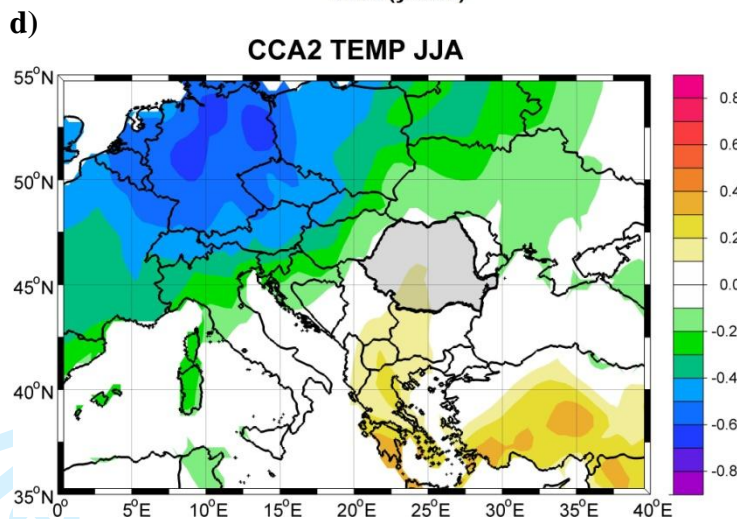
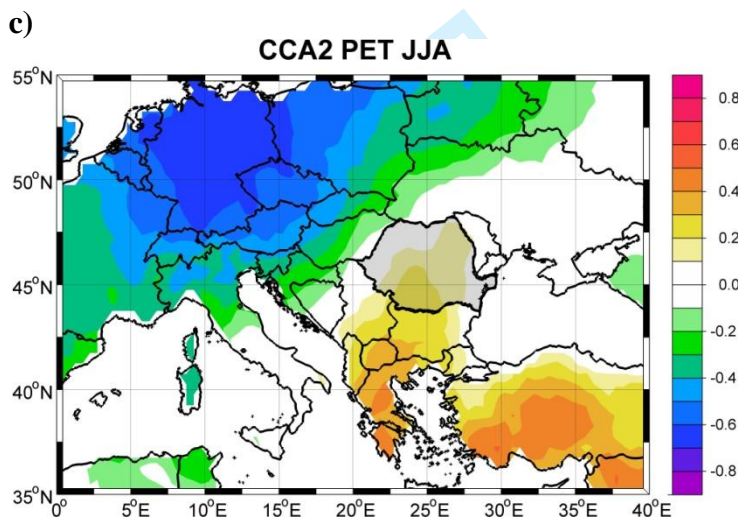
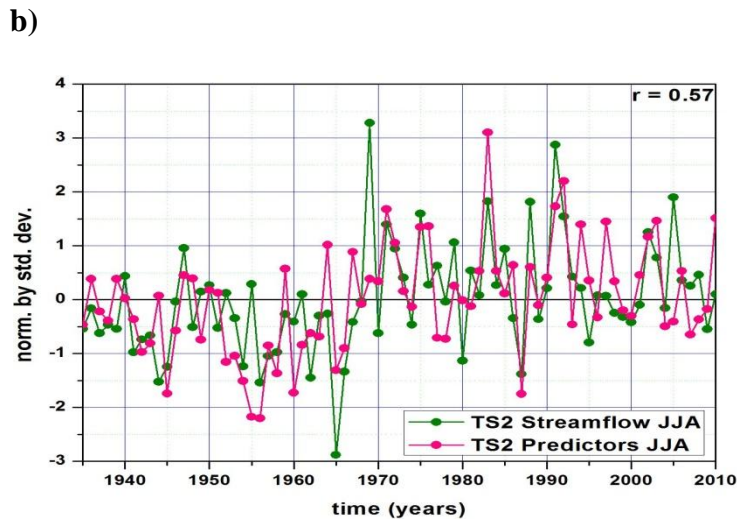
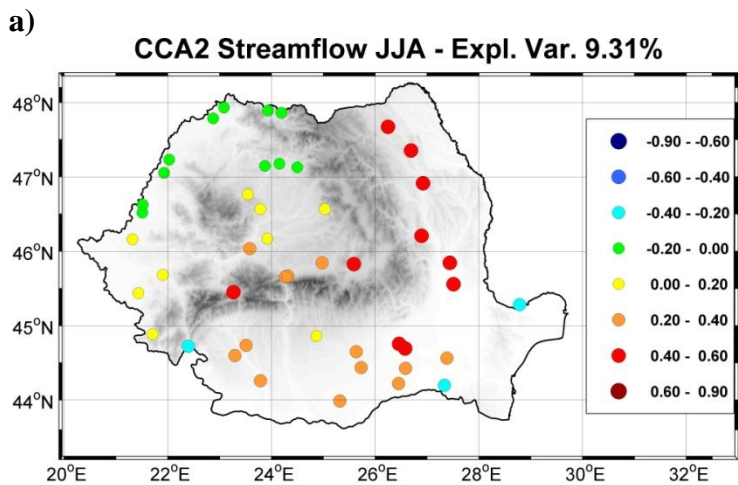
The summer percent from the annual mean streamflow





Only

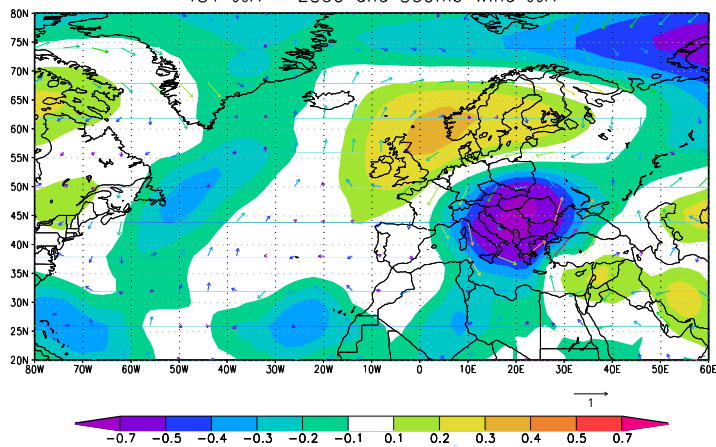






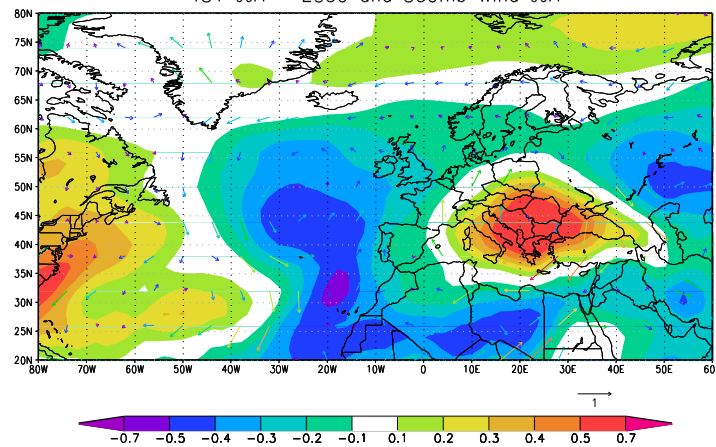
a)

High Composite Map  
TS1 JJA - Z850 and 850mb Wind JJA



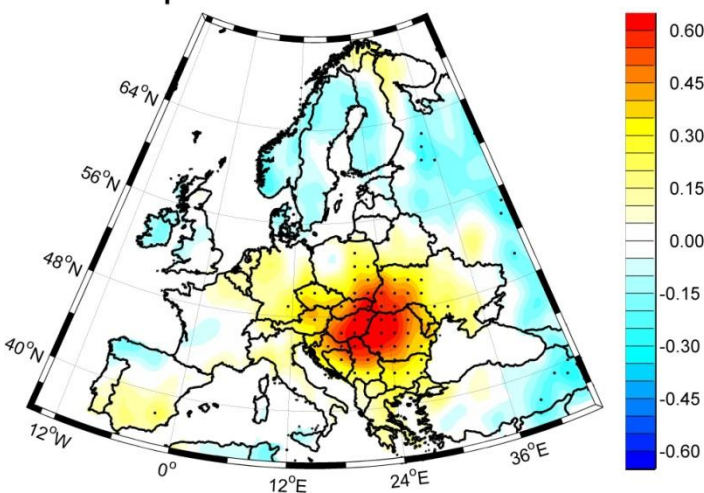
b)

Low Composite Map  
TS1 JJA - Z850 and 850mb Wind JJA



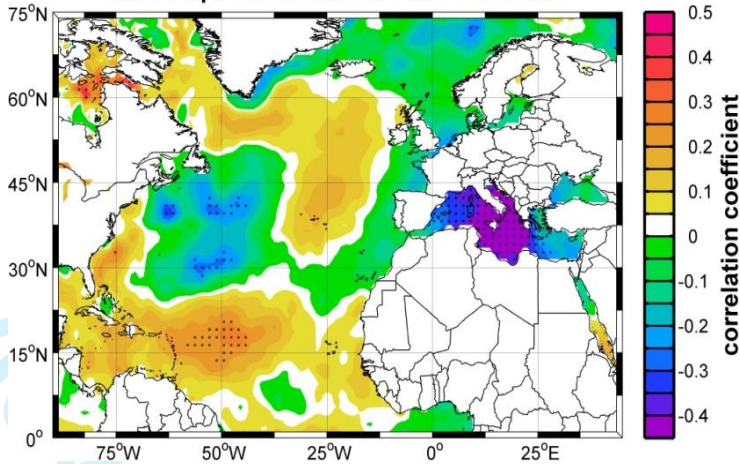
c)

Corr. Map: TS1 Streamflow JJA - PP JJA



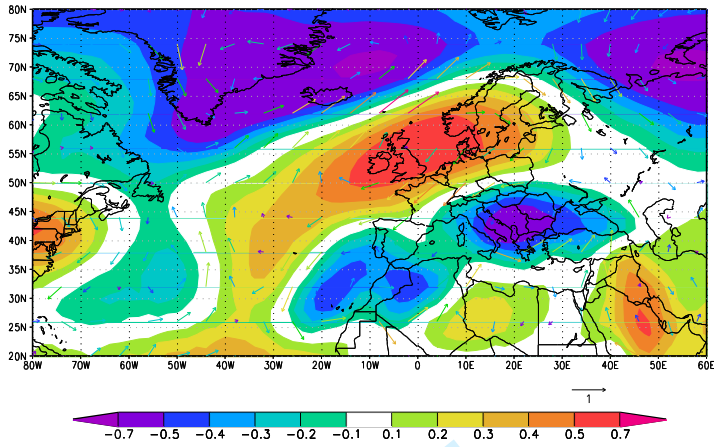
d)

Corr. Map: TS1 Streamflow JJA - SST JJA



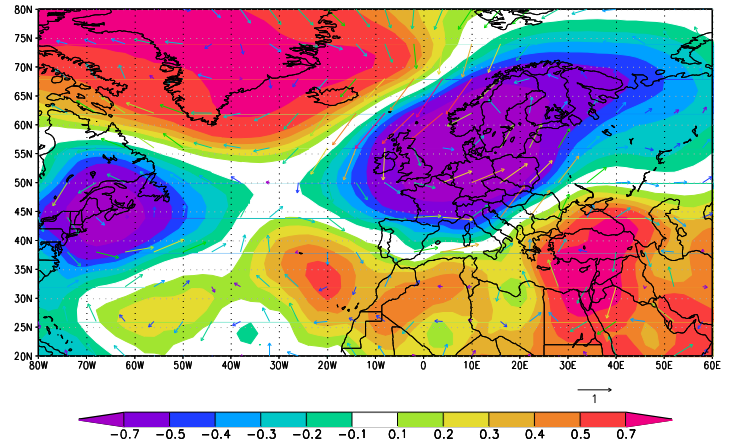
a)

High Composite Map  
TS2 JJA - Z850 and 850mb Wind JJA



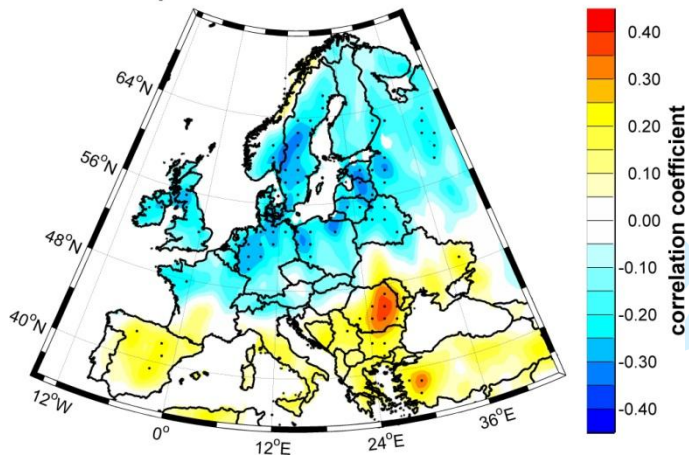
b)

Low Composite Map  
TS2 JJA - Z850 and 850mb Wind JJA



c)

Corr. Map: TS2 Streamflow JJA - PP JJA



d)

Corr. Map: TS2 Streamflow JJA - SST JJA

